CHAPTER 6

ELECTROCHEMICAL MODEL FOR CARBON-NANOTUBE DUAL-GATED ENFET (CNT-DG-ENFET) WITH HfO_2 AS DIELECTRIC FOR ACETYLCHOLINE DETECTION

CHAPTER 6

Electrochemical model for carbon-nanotube dual-gated ENFET (CNT-DG-ENFET) with HfO_2 as dielectric for acetylcholine detection

6.1. An overview on CNT-DG-ENFET

CNT-DG-ENFET is a dual gated ENFET device in which carbon nanotube is the substrate semiconductor material having dual gates: one electrolytic and the other metal gate. This chapter deals with the electrochemical modeling of chitosan/nickel oxide (CH/NiO) based CNT-DG-ENFET with HfO_2 as dielectric for acetylcholine detection. The schematic of the fabricated CNT-DG-ENFET has been shown in Fig. 6.1. It consists of ITO coated glass plate as substrate, ZnO as bottom insulator, polyethylene imine (PEI) doped carbon nanotube as n-type channel, drain and source regions (structure shown in Chapter 2), HfO_2 as top gate insulator and chitosan/nickel oxide (CH/NiO) nanocomposite as sensing membrane arranged from bottom to top respectively. The structure of formation of CH/NiO composite with HfO_2 and CNT has been shown in Fig. 6.2. It clearly describes the bonding between different elements of the layer. The biocompatibility and chemical stability of NiO is very high which makes it a promising material in nanobiosensing. It also has other unique and efficient properties like electro catalysis and high electron transfer [3, 91]. When NiO forms a composite with CH, it gives a highly biocompatible layer with excellent film forming capability and mechanical strength [9].

CNTFET reduces threshold voltage and enhances small ON-OFF current ratio because of its high mobile charge carriers and low internal contact resistance [20]. The dual gated feature enhances the sensitivity of the device [95]. The fabrication and experimental details of the device has been explained in details in reference [7]. Since, values of parameters used for modeling this device are to be extracted mostly from parameters used for fabrication of the device and the experimental results, a brief description of its fabrication process and the experimental part are highlighted in the next section.

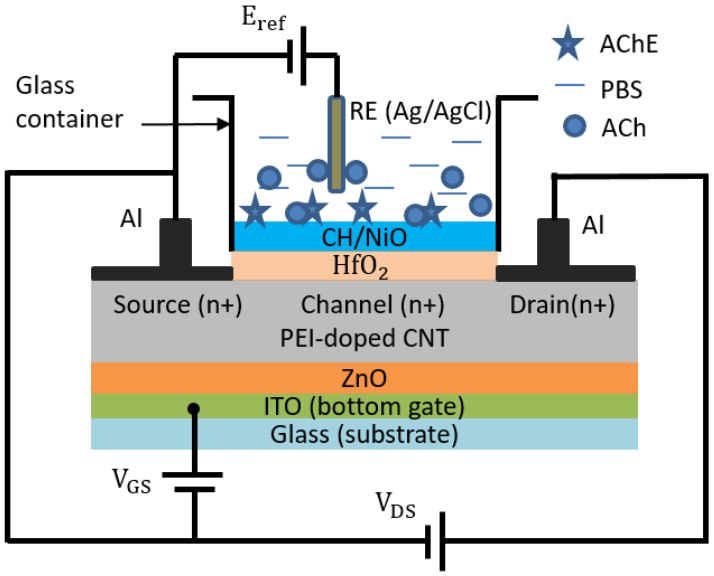

Fig. 6.1. Schematic of fabricated CNT-DG-ENFET for Acetylcholine Detection [7]

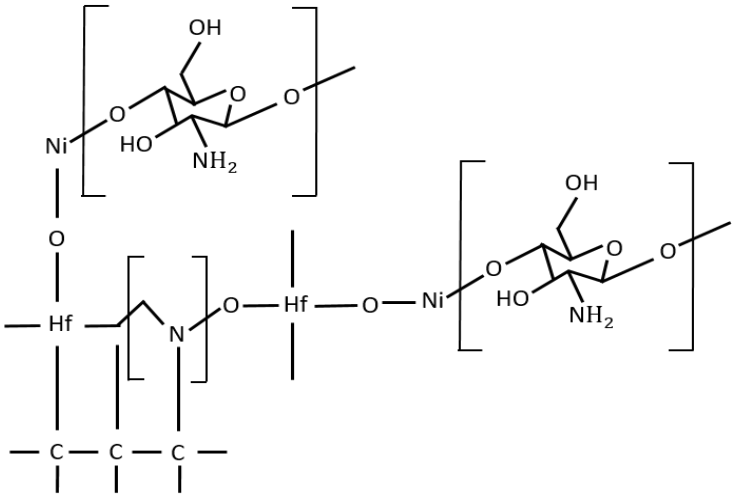

Fig. 6.2. Structure of CH/NiO composite with HfO_2 and CNT [7]

6.2. Fabrication and characterization of CNT-DG-ENFET

The structure of CNT-DG-ENFET is almost similar to the CNT-ENFET discussed in Chapter 5 except using HfO_2 as top gate dielectric and dual gate. So, most of the fabrication steps are similar. The device consists of ITO coated glass having dimension ~5 mm × 2 mm as substrate, which is a conducting material and used as working

electrode in the three electrode electrochemical deposition of other layers. On its top, zinc oxide (ZnO) with dimension ~5 mm × 2 mm × 10 nm is deposited as bottom gate insulator, which provides smaller contribution of drain current by bottom gate than top gate due to its low dielectric constant (~ 1.5). CNT is doped with polyethylene imine (PEI) to make it n-type and deposited using ECD technique over ZnO. This CNT acts as channel along with source and drain regions. The dimension of source as well as drain is ~5 mm × 2 mm × 100 nm and dimension of channel is 1 mm × 2 mm × 100 nm. Prior to being used, CNT has been prepared using catalytic chemical vapor deposition (CVD) technique [60] and functionalized using boiling acid treatment technique [26]. For CNT solution, 10 mg CNT has been dispersed in 10 ml methanol and sonicated for several minutes. Then, 5 ml solution of PEI has been added to this CNT solution. On top of CNT, HfO_2 layer with dimension ~1 mm × 2 mm × 10 nm has been deposited as top gate insulator using ECD technique. HfO_2 has a very high dielectric constant (~25) leading to reduction in direct tunneling leakage current and improved device performance. It is also compatible with the nanomaterials and thereby, facilitates device miniaturization. For preparation of HfO_2 layer, 100 mg solid $HfCl_4$ has been dissolved in 10 ml de–ionized water and sonicated for several minutes [97, 98]. Solid $HfCl_4$ has been used here since HfO_2 is insoluble in water. Then, it was deposited on the top of the channel region by using solution process and heated at temperature of 180 ºC for getting dry layer of HfO_2. Thickness of HfO_2 layer has been measured by using gravimetric analysis technique and found to be ~10 nm. As it is difficult to immobilize the enzyme AChE on top of HfO_2, a highly biocompatible layer composed of chitosan and NiO (CH/NiO) is therefore, deposited on top of the HfO_2 layer and it acts as enzyme sensing membrane. The enzyme acetylcholine esterase (AChE) is immobilized on the CH/NiO sensing membrane by physical adsorption technique [51].

Now, to show the behavior of CNT-DG-MOSFET outside the liquid: aluminum metal has been deposited on the top of the HfO_2 layer (by filament evaporation technique) that acts as the gate of MOSFET forming CNT-DG-MOSFET. Dc drain current has been recorded at different gate voltages using DMM. Drain currents have been plotted against drain voltages from 0 to 1 V, in step of 0.2 V with applied top gate voltages (i.e. reference voltage) from 0 to 1 V, in step of 0.2 V as shown in Fig. 6.3. The bottom gate voltage has been fixed at 0.6 V. The transfer characteristic curve has been drawn (for

V_{DS} = 0.3 V) as shown in Fig. 6.4. The threshold voltage from the transfer characteristic curve has been obtained by using ELR technique and found as ~ 0.17V.

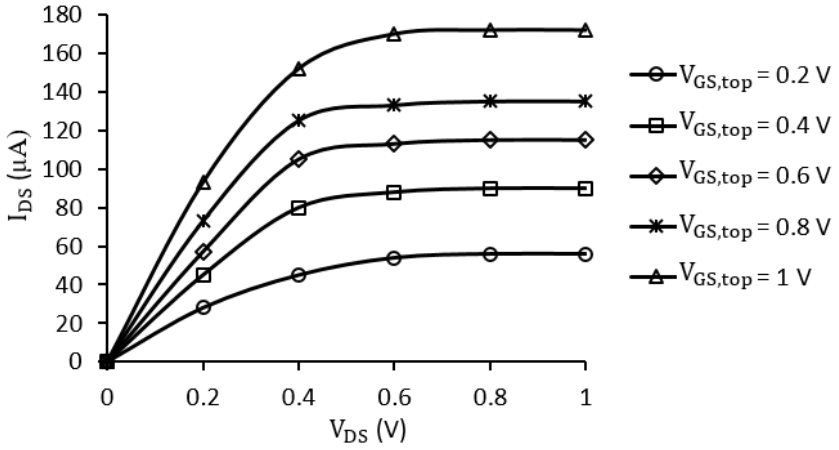

Fig. 6.3. Output characteristics of CNT-DG-MOSFET

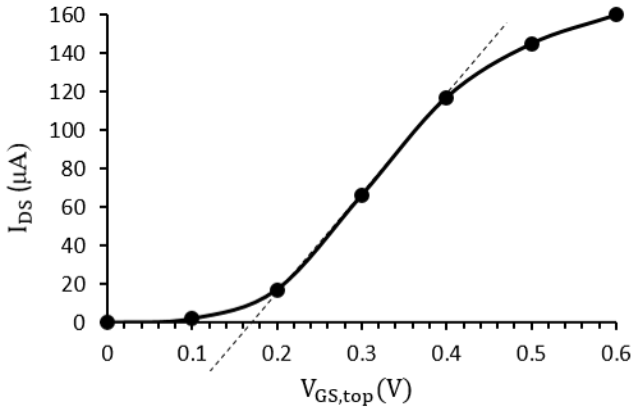

Fig. 6.4. Transfer characteristics of CNT-DG-MOSFET

For in liquid measurements (CNT-DG-ENFET): 1 µL of enzyme AChE (prepared as discussed in Chapter 5) is immobilized on the sensing membrane by using physical adsorption technique [88]. The device is dried overnight and stored in refrigerator at 4 ^{o}C, when not in use. Output characteristics of the CNT-DG-ENFET has been obtained by plotting drain voltage vs drain current for ACh concentration from 0.01 to 0.2 mM at a fixed reference voltage of 0.6 V as shown in Fig. 6.5. It has been observed that

when drain voltage reaches at 0.4 V, saturation occurs in drain current like characteristics of a FET. Fig. 6.6 shows V_{GS} vs I_{DS} plot for ACh solution having pH 6 and 6.5 for V_{DS} = 0.4 V.

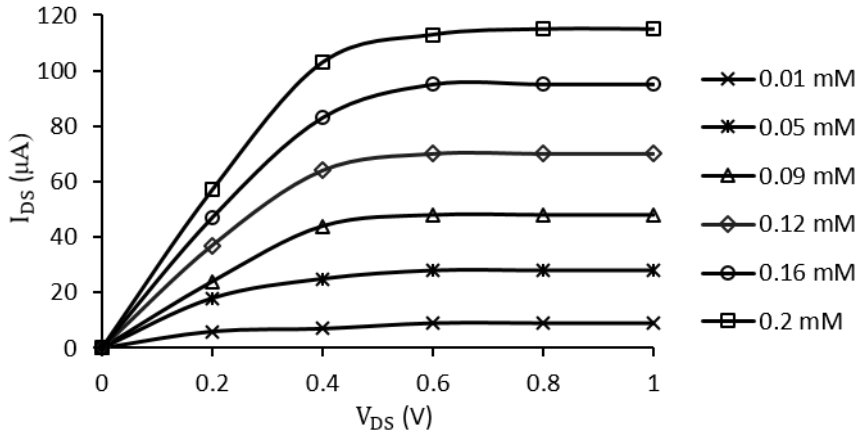

Fig. 6.5. Output characteristics of CNT-DG-ENFET

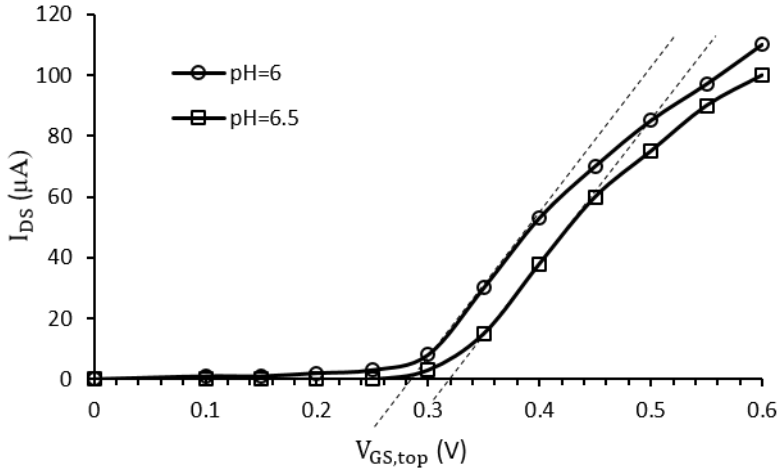

Fig. 6.6. Transfer characteristics of CNT-DG-ENFET

6.3. CNT-DG-ENFET MODEL

An electrochemical model of the fabricated device has been developed. The modeling has been done considering each layer of the device as discussed in Chapter 5 with variations in the current transport model due to use of dual gate and HfO_2 as dielectric

material. The different layers of the device along diffusion length (x) has been shown in Fig. 6.7.

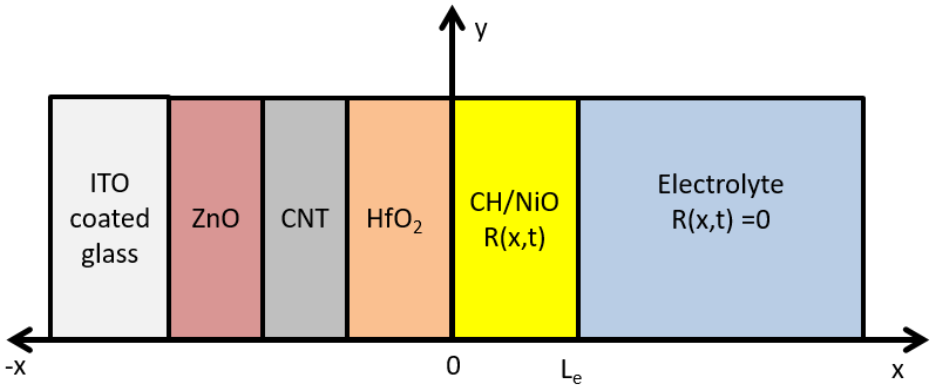

Fig. 6.7. Description of CNT-DG-ENFET structure with respect to diffusion length (x)

6.3.1. Modeling pH variations in CNT-DG-ENFET due to acetylcholinesterase enzymatic reactions and diffusion phenomena

The modeling of acetylcholinesterase enzymatic reactions, diffusion of acetylcholine and acetic acid in PBS solution and pH variations due to release of H^+ions have been discussed in details in Chapter 5. In CNT-DG-ENFET, HfO_2 has been used as gate dielectric instead of ZrO_2. The effect of use of HfO_2 can be seen in the surface potential variations because its pH_{pzc} is different from ZrO_2.

The plot for substrate and product concentration variation with diffusion length following the diffusion model has been shown in Fig. 6.8. The increase in product concentration in the enzyme sensing layer leads to the increase in formation of H^+ ions. These H^+ions affects the pH of the electrolyte in the enzyme sensing layer. The pH is seen to decrease with increase in product concentration as shown in Fig. 6.9. The pH of the buffer electrolyte is initially kept at 7, so, as the product formation starts the pH gradually decreases from the enzyme electrolyte interface towards the enzyme insulator interface.

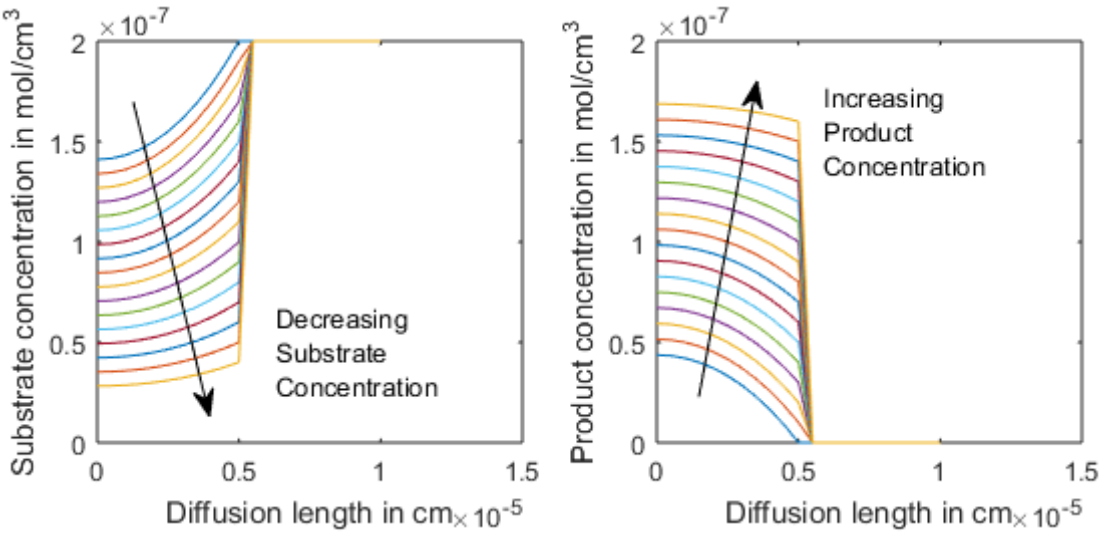

Fig. 6.8. Substrate and product concentration variation with diffusion length at different time

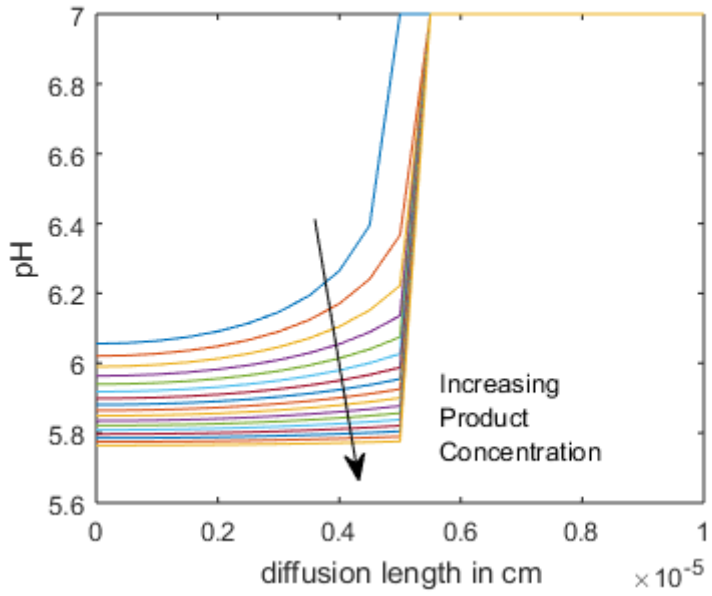

Fig. 6.9. Diffusion length vs pH with increasing product concentration

Fig. 6.10 shows the pH variation with product concentration for diffusion length from 0 to L_e. Closer to L_e, the pH of the electrolyte is almost 7 as no reactions occur there. Going deeper when $x < L_e$, the pH gradually decreases and finally becomes constant when no more product is formed.

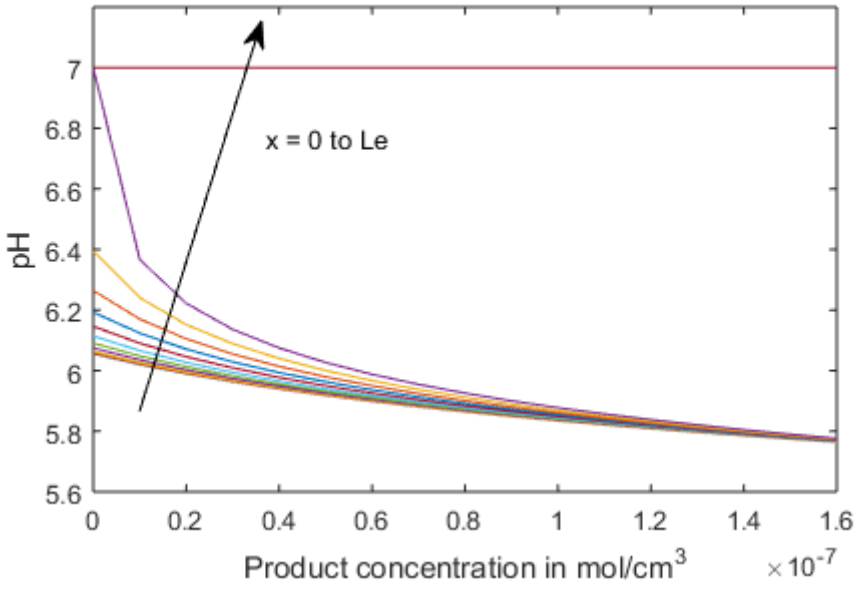

Fig. 6.10. Product concentration vs pH with varying diffusion length

6.3.2. Current transport model for CNT-DG-ENFET

In dual gated ENFET, top and bottom gates are present which together affect the current flowing through the device. Therefore, the current flow due to both the gates is added up to get the total current. The total drain current in the linear and saturation region for dual gated ENFET are given by Eqs. (6.1) and (6.2) respectively [66, 94].

$$I_{DS,lin,dual} = \mu \frac{W}{L} V_{DS}\left[C_{ox,top}\left\{\left(V_{GS,top} - V_{TH,top}\right) - 0.5\, V_{DS}\right\} + C_{ox,bottom}\left\{\left(V_{GS,bottom} - V_{TH,bottom}\right) - 0.5\, V_{DS}\right\}\right] \quad (6.1)$$

$$I_{DS,sat,dual} = \mu \frac{W}{2L}\left[C_{ox,top}\left(V_{GS,top} - V_{TH,top}\right)^2 + C_{ox,bottom}\left(V_{GS,bottom} - V_{TH,bottom}\right)^2\right] \quad (6.2)$$

In the above equation $C_{ox,top}$ and $C_{ox,bottom}$ are the capacitances and $V_{TH,top}$ and $V_{TH,bottom}$ are the threshold voltages for the top and bottom gates respectively.

$$C_{ox,top} = \frac{\kappa_{ox,top} \cdot \varepsilon_0}{t_{ox,top}} \quad (6.3)$$

$$C_{ox,bottom} = \frac{\kappa_{ox,bottom} \cdot \varepsilon_0}{t_{ox,bottom}} \tag{6.4}$$

where, $\kappa_{ox,top}$ and $\kappa_{ox,bottom}$ are the dielectric constants and $t_{ox,top}$ and $t_{ox,bottom}$ are the thickness of the top and bottom gate insulators respectively. The $\kappa_{ox,bottom} \ll \kappa_{ox,top}$ and $t_{ox,bottom} \geq t_{ox,top}$, so, $C_{ox,bottom} \ll C_{ox,top}$. It indicates that the current contribution by bottom gate is lesser than top gate. The top gate parameter variation acts as input, so, its effect is more prominent as compared to bottom gate with the use of high-κ dielectric material.

In case of dual gated ENFET, two threshold voltage arises because of top and bottom gate respectively. As the top gate of the device forms an ISFET structure so, $V_{TH,top}$ is represented by ISFET's threshold voltage equation with exclusion of $2\Phi_f$ factor. The bottom gate acts like simple MOSFET gate and so, $V_{TH,bottom}$ is represented by general threshold voltage equation of MOSFET with no $2\Phi_f$ term.

$$V_{TH,top} = E_{ref} - \psi_0 + \chi_{sol} - \frac{\Phi_{CNT}}{q} - \frac{Q_{ox,top} + Q_{ss,top} + Q_{CNT}}{C_{ox,top}} \tag{6.5}$$

$$V_{TH,bottom} = \frac{\Phi_M - \Phi_{CNT}}{q} - \frac{Q_{ox,bottom} + Q_{ss,bottom} + Q_{CNT}}{C_{ox,bottom}} \tag{6.6}$$

where, $Q_{ox,top}$ and $Q_{ox,bottom}$ are the top and bottom gate insulator charge respectively; $Q_{ss,top}$ and $Q_{ss,bottom}$ are the insulator CNT interface charge for top and bottom gates respectively; Φ_M is the work function of bottom gate material.

Now, the change in pH results in $\psi_{0,CNT-DG-ENFET}$ variation as given by Bousse's model in Eq. (2.13) of Chapter 2. Surface potential increases with a decrease in pH as shown in Fig. 6.11A. The sensitivity of the HfO_2 insulating material is found to be very high because of which small variations in pH results in considerable potential variations, which can be detected by the device.

Fig. 6.11B shows a variation in top gate threshold voltage with pH as depicted in Eq. (6.5). The bottom gate threshold voltage is almost constant. The top gate threshold voltage decreases with decrease in pH. This varying voltage serves as the input parameter for the variation in drain current. Fig. 6.12 shows a comparison between the

modeling and experimental results in terms of output drain current with drain to source voltage at different acetylcholine concentrations. A good fit is seen between the two plots.

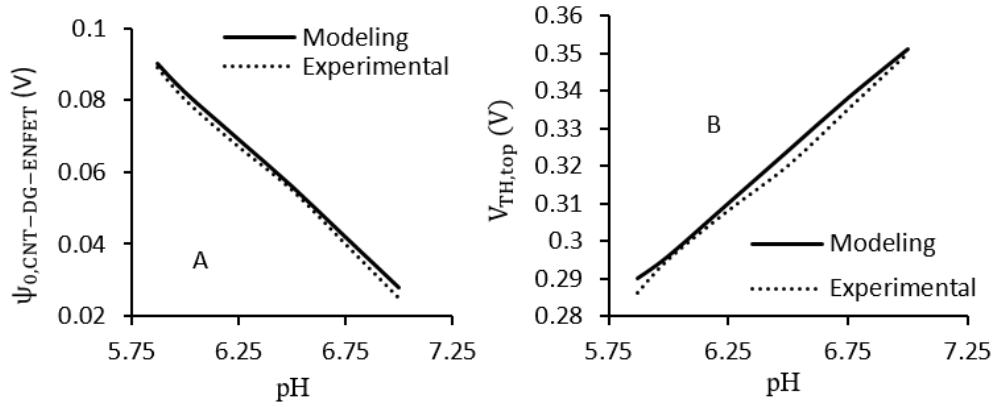

Fig. 6.11. (A) pH vs $\psi_{0,CNT-DG-ENFET}$ plot showing comparison between modeling and experimental data. (B) pH vs $V_{TH,top}$ plot showing comparison between modeling and experimental data.

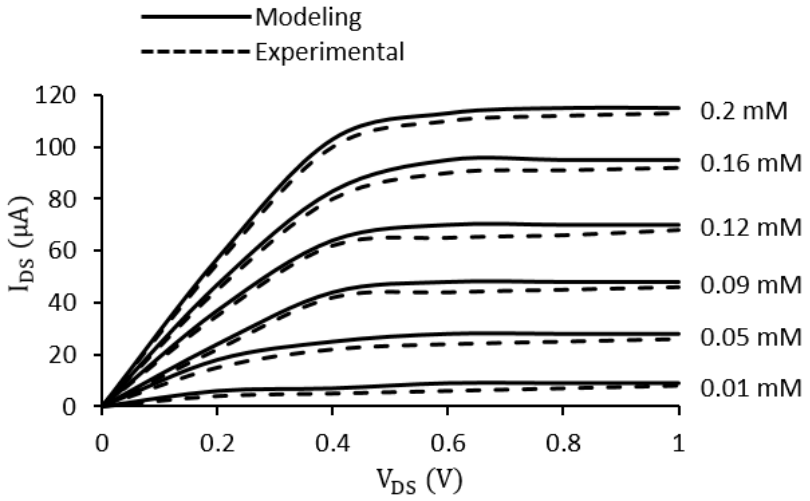

Fig. 6.12. Output characteristics of CNT-DG-ENFET showing comparison between modeling and experimental results

6.3.3. Dual Gate pH Sensitivity

The top gate sensitivity (S_{top}) of the device is determined from Eq. (6.7) using the Bousse's model in terms of V/pH. But the ENFET device discussed here is dual gated. Hence, both the gates influence the pH sensitivity of the device [94]. The total device sensitivity is given by Eq. (6.8). It depends on the top and bottom gate capacitances. Higher the top gate capacitance compared to bottom gate, higher is the sensitivity of the device. So, a dielectric having higher κ is used as top gate as compared to bottom gate.

$$S_{top} = \left(\frac{2.303kT}{q}\right)\left(\frac{\beta}{\beta+1}\right) \tag{6.7}$$

$$S_{dual} = \frac{C_{\text{ox,top}}}{C_{\text{ox,bottom}}} S_{top} \tag{6.8}$$

The sensitivity of the device was found to be about 1.1 V/pH, which is comparable to experimentally determined sensitivity of 1.2 V/pH. This enhanced sensitivity is due to use of dual gate. Values of various parameters that were found much influential during simulation are tabulated in Table 6.1.

6.4. Summary

The CNT based dual gated ENFET model has been developed for acetylcholine detection using the enzymatic reactions, diffusion phenomena, acid/base reactions, pH detection properties of ISFET and current transport model of dual gated CNTFET. The ISFET consists of HfO_2 as gate insulator on top of CNT substrate. HfO_2 is a high-κ dielectric with dielectric constant 25 and has thickness of about 10 nm giving good insulating effect and enhanced sensitivity even at nanometer range. The use of ZnO, a low-κ dielectric, as the bottom gate material gives lesser current as compared to the top gate. Because of this the variation in current mostly occurs because of top gate. The NiO/CH composite in which the enzymes are immobilized has larger area and lesser thickness of about 50 nm. As a result, it can hold more enzymes, give better response time and higher sensitivity. The mobility of CNT is very high which also contributes towards the high sensitivity of the device as even very small potential variation at the

surface gives a noticeable change in current. The results of the model has shown good agreement with the experimental results. The use of dual gate has raised the sensitivity beyond Nerstian limit.

Table 6.1: Values of various parameters considered for CNT-DG-ENFET modeling

Sl. No.	**Parameter**	**Values**
1.	Dielectric constant for HfO_2 $(\kappa_{ox,top})$	25
2.	Dielectric constant for ZnO $(\kappa_{ox,bottom})$	1.5
3.	Thickness of HfO_2 $(t_{\mathrm{ox,top}})$	10 nm
4.	Thickness of ZnO $(t_{\mathrm{ox,bottom}})$	10 nm
5.	pH of PBS solution (pH_0)	7
6.	Reference Voltage (E_{ref})	0.6 V
7.	Average work function of CNT (ϕ_{CNT})	4.7 eV
8.	Surface dipole potential of the solvent (χ_{sol})	0.3 V
9.	Number of charge carriers present in CNT (n_{CNT})	9×10^{15} cm^{-3}
10.	Length of CNT (L_{CNT})	5 mm
11.	Work function of ITO (ϕ_M)	4.6 eV
12.	CH/NiO thickness (L_e)	50 nm
13.	Electron mobility of CNT (μ)	10000 cm^2/Vs
14.	Width of channel (W)	2 mm
15.	Length of channel (L)	1 mm